

pubs.acs.org/chemneuro Research Article

Hippocampal Commissural Circuitry Shows Asymmetric cAMP-**Dependent Synaptic Plasticity**

Lukas Faiss, Aikaterini Salivara, Silvia Oldani, Jörg Breustedt, Dietmar Schmitz,* and Benjamin R. Rost*



Cite This: ACS Chem. Neurosci. 2025, 16, 4236-4245



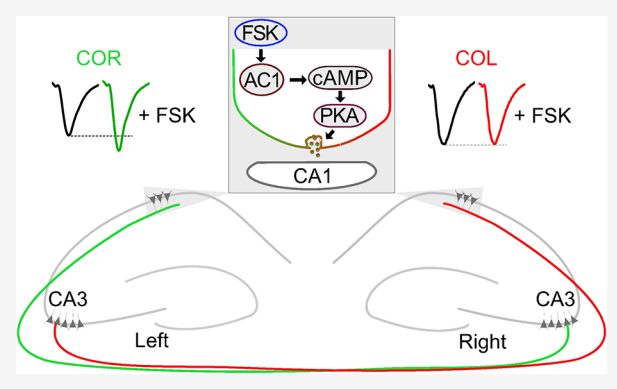
ACCESS I

Metrics & More

Article Recommendations

s Supporting Information

ABSTRACT: Hemispheric asymmetries in NMDAR-dependent synaptic plasticity have been described in hippocampal area CA1, but it remains unclear whether similar lateralized mechanisms exist for cyclic adenosine monophosphate (cAMP)-dependent plasticity. Here, we investigated whether cAMP-mediated potentiation of synaptic transmission in mouse CA1 exhibits hemisphere-specific properties. In recordings with electrical stimulation of CA1 inputs, a subset of recordings in the left, but not in the right hemisphere CA1, exhibited a pronounced cAMP-induced potentiation of field excitatory postsynaptic potentials (fEPSPs). To isolate input-specific contributions, we expressed the optogenetic actuator ChrimsonR unilaterally in the CA3/CA2 region of wild-type mice. Light-evoked glutamate release from ipsilateral Schaffer collaterals showed no cAMP sensitivity in either



hemisphere, while commissures originating from the right (COR) exhibited cAMP-mediated potentiation of transmission in a subset of experiments. Notably, this effect was absent at commissures originating from the left (COL). The selective presence of the effect prompted us to further investigate the underlying cell population using CA3-specific (G32-4 Cre) and CA2-specific (Amigo2-Cre) driver lines. Recordings from synapses of CA3 COR recapitulated the cAMP-induced potentiation of transmitter release observed in wild-type animals. However, the effect was again restricted to a subset of experiments, did not correlate with the age or the sex of the mice, and was absent in recordings with specific stimulation of CA2 COR. Our results demonstrate a variable cAMP sensitivity of synaptic transmission at COR synapses in the left CA1. Altogether, we reveal a hemisphere-specific cAMP-mediated synaptic plasticity at CA3 COR onto CA1, underscoring hidden heterogeneity and lateralization in hippocampal circuit function.

KEYWORDS: hippocampus, commissural fibers, lateralization, cAMP, synaptic plasticity

INTRODUCTION

Within the hippocampus, CA1 pyramidal neurons receive glutamatergic input from both ipsilateral Schaffer collaterals and contralateral commissural projections, both originating from CA3 and CA2 pyramidal neurons.¹⁻³ As Schaffer collaterals and commissural fibers share similar targets in the CA1 stratum radiatum, their overlapping distributions complicate selective stimulation.⁴ Despite the mirror-image wiring at the macroscopic level, CA1 inputs appear to exhibit lateralized, hemispheric-specific functional differences. In mice, CA1 pyramidal cell synapses show input-specific expression of ionotropic glutamate receptors. Synapses with presynaptic terminals originating from the right hippocampus predominantly express GluA1-containing AMPA receptors, whereas synapses with input from the left hippocampus show higher expression levels of GluN2B-containing NMDA receptors. 5,6 In inversus viscerum (iv) mice, hemispheric asymmetry is absent. This lack of lateralization is linked to deficits in learning and memory, including slower spatial learning and reduced working memory performance.^{7,8} Gene expression analyses revealed greater transcriptional changes in the right

hippocampus following spatial learning.9 Additionally, disrupting interhemispheric connections uncouples gamma wave synchronization, suggesting that the right hippocampus leads bilateral information before cortical transmission. 10 Hemispheric asymmetries also influence synaptic plasticity. NMDAR-dependent long-term potentiation (LTP) at CA1 synapses was suggested to be preferentially induced by left CA3 inputs, implicating a dominant role of the left hemisphere in driving postsynaptic LTP. 11-13 Furthermore, commissural projections from CA2/3 in the left hemisphere are essential for full postsynaptic plasticity and place field formation in CA1.¹⁴ While some findings support this left-dominant model, its generality across species and conditions remains debated. 15,16 Beside the classical NMDA receptor/CaMKII-dependent

June 16, 2025 Received: Revised: September 18, 2025 Accepted: October 6, 2025 Published: October 13, 2025





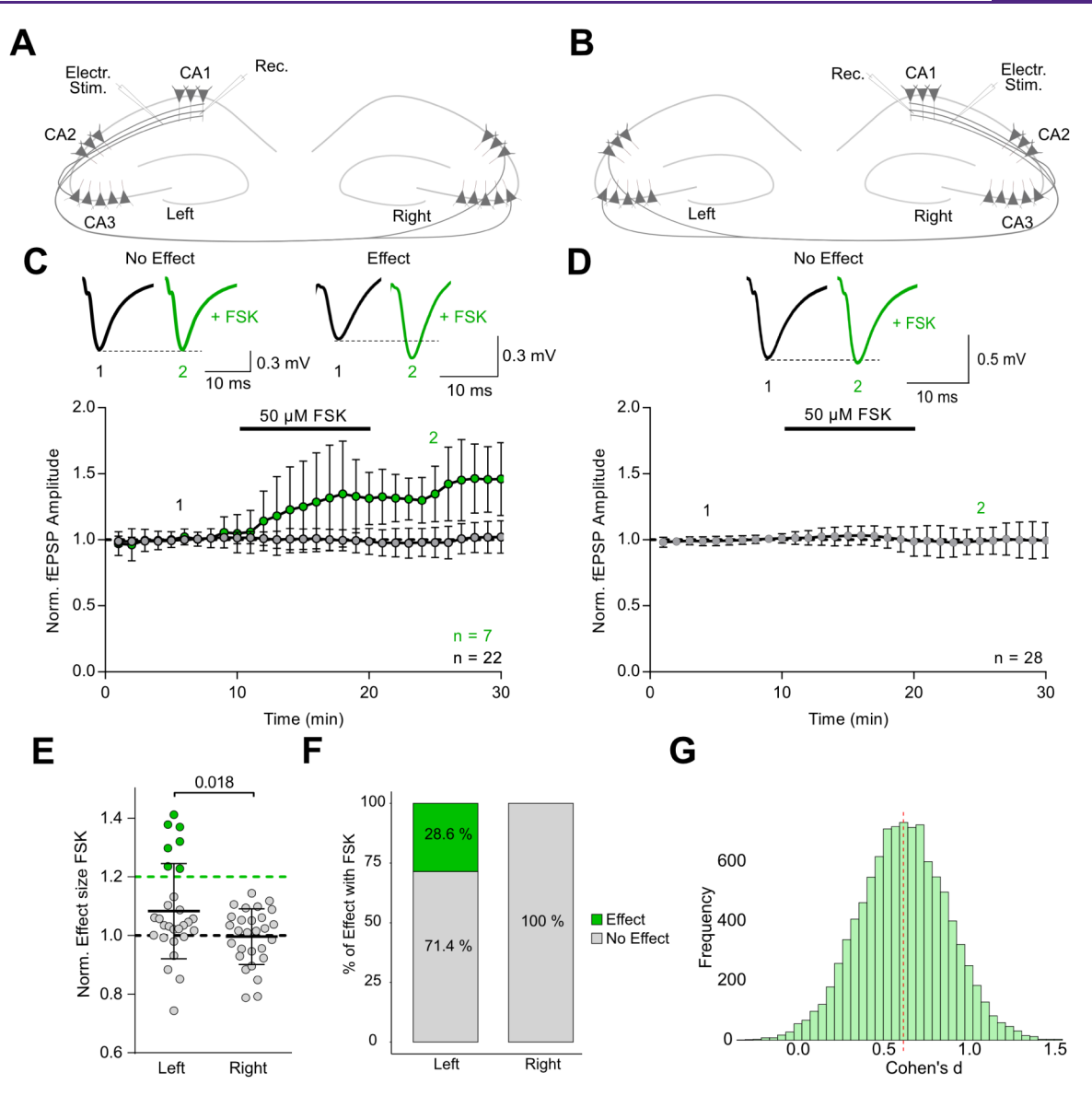


Figure 1. Selective potentiation of synaptic responses by forskolin in the left hippocampus. A, B Schematic of the field stimulation and recording setup in the CA1 region of the left (A) and right (B) hippocampus. C, D Representative traces and time courses of electrically evoked fEPSPs recorded in the left (C) and right (D) hippocampus. Black traces represent average of a 10 min baseline; green traces show responses after application of 50 μ M forskolin (FSK). The averages of the recordings with an FSK-effect >20% are shown in green, while the averages of all other recordings are shown in gray (mean \pm SD). E Summary of FSK effects on normalized fEPSP amplitudes reveals significantly greater potentiation in the left hemisphere compared to the right (left: $108.3\% \pm 16.3\%$; right: $99.6\% \pm 9.5\%$; p = 0.018, unpaired t test with Welch's correction). F Percent stacked bar plot indicating the distribution of recordings with and without significant potentiation, based on a 20% threshold (Left: 28.6% of recordings showed an effect, 71.4% no effect; Right: 0% with effect). G Histogram of bootstrapped Cohen's d values comparing left and right hemisphere recordings, revealing a medium effect size favoring the left hemisphere (Cohen's d = 0.664).

signaling cascade, cAMP-dependent pathways represent additional mechanisms for inducing or supporting both pre- and postsynaptic forms of plasticity. Here, we investigated whether Schaffer collateral or commissural CA3-CA1 synapses exhibit hemisphere-specific cAMP-dependent potentiation of synaptic transmission. Using optogenetics and electrophysiological recordings, we tested whether pharmacological cAMP modulation differentially affects synaptic plasticity in CA1. Using optogenetics and electrophysiological recordings, we tested whether pharmacological cAMP modulation differentially affects synaptic plasticity in CA1.

RESULTS

Asymmetrical cAMP Modulation of Hippocampal CA1 Inputs. Pharmacological enhancement of cAMP signaling has previously been reported to increase synaptic input to CA1 pyramidal neurons by approximately 20%. To assess whether this modulation differs across hemispheres or specific input pathways, we defined a >20% increase in synaptic transmission following bath application of 50 μ M forskolin (FSK), a pharmacological activator of adenylyl cyclases, as a threshold for a positive cAMP effect. Using this criterion, we examined hemisphere-specific responses by recording field excitatory postsynaptic potentials (fEPSPs) in area CA1 of both the left and right hippocampus (Figure 1A,B). In the left hippocampus, a subset of recordings exhibited potentiation

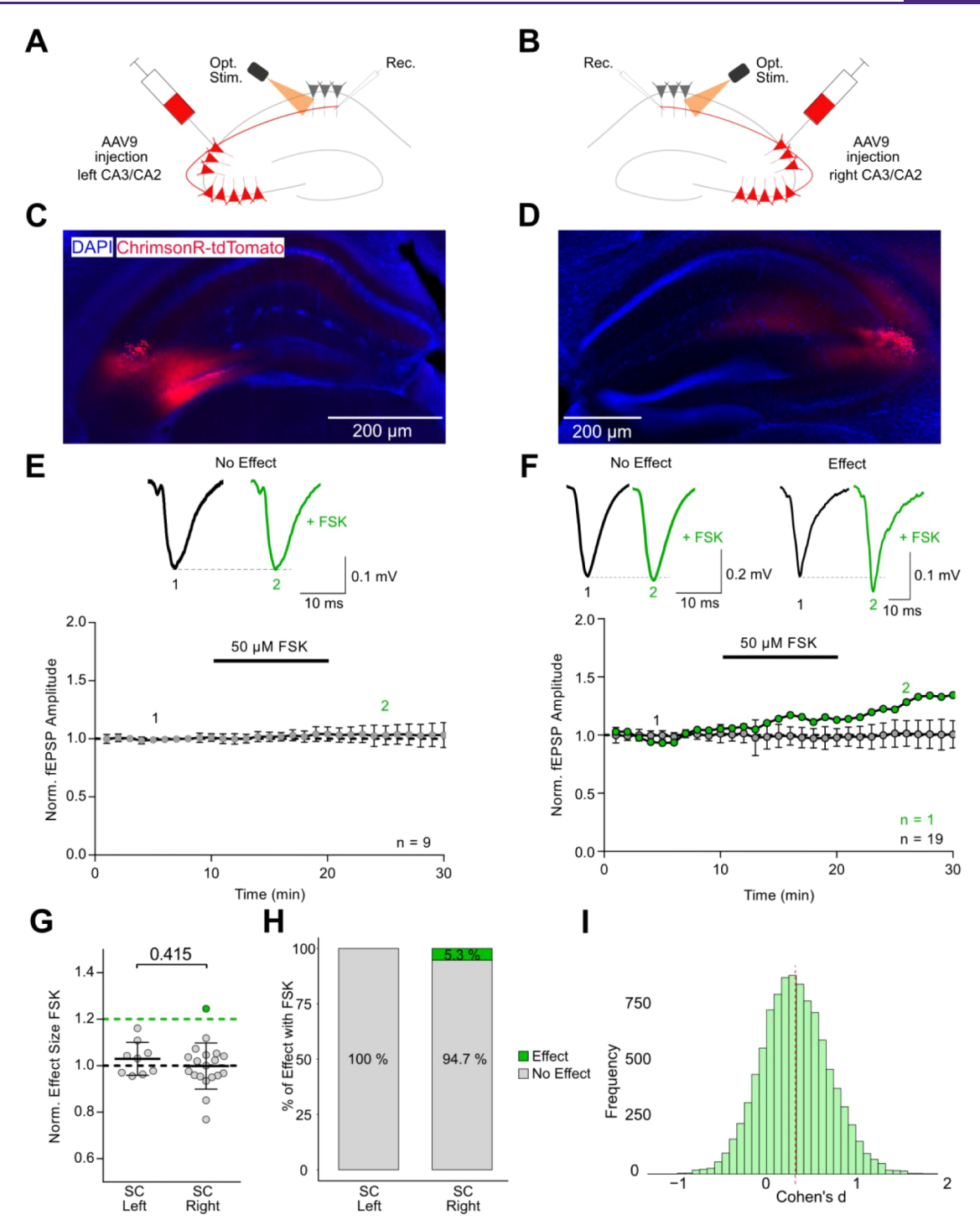


Figure 2. No FSK effect on Schaffer collateral transmission evoked by optogenetic stimulation. A, B Experimental configuration for selective optogenetic stimulation of Schaffer collateral inputs with recordings from the CA1 region in the left (A) or right (B) hippocampus. C, D Fluorescent micrographs showing ChrimsonR-tdTomato expression in the CA3/CA2 region in the left (C) or right (D) hippocampus. DAPI staining labels cell nuclei. E, F Representative optogenetically evoked fEPSP traces from the left (E) and right (F) hippocampus. Black traces represent baseline responses; green traces show post-FSK responses. Time courses from the left (E) and right (F) hippocampus. Time course plots distinguish effect recordings (>20% increase, green) from noneffect recordings (gray). G Group summary of normalized fEPSP amplitudes shows no significant difference in FSK-induced potentiation between hemispheres (p = 0.415, unpaired t test; SC = Schaffer Collaterals). H Percent stacked bar plot categorizing individual recordings based on presence or absence of a >20% increase in synaptic strength. No recordings from the left hemisphere met this criterion, while 1 out of 20 recordings (5.3%) in the right hemisphere showed an effect. I Distribution of bootstrapped Cohen's d values comparing left and right hemisphere responses indicates a small effect size (Cohen's d = 0.354), indicating a minor hemispheric difference.

(>20% increase), whereas recordings from the right hemisphere consistently failed to meet this threshold. Specifically, 7

out of 29 recordings in the left hemisphere (28.6%) showed a significant FSK-induced increase in synaptic transmission

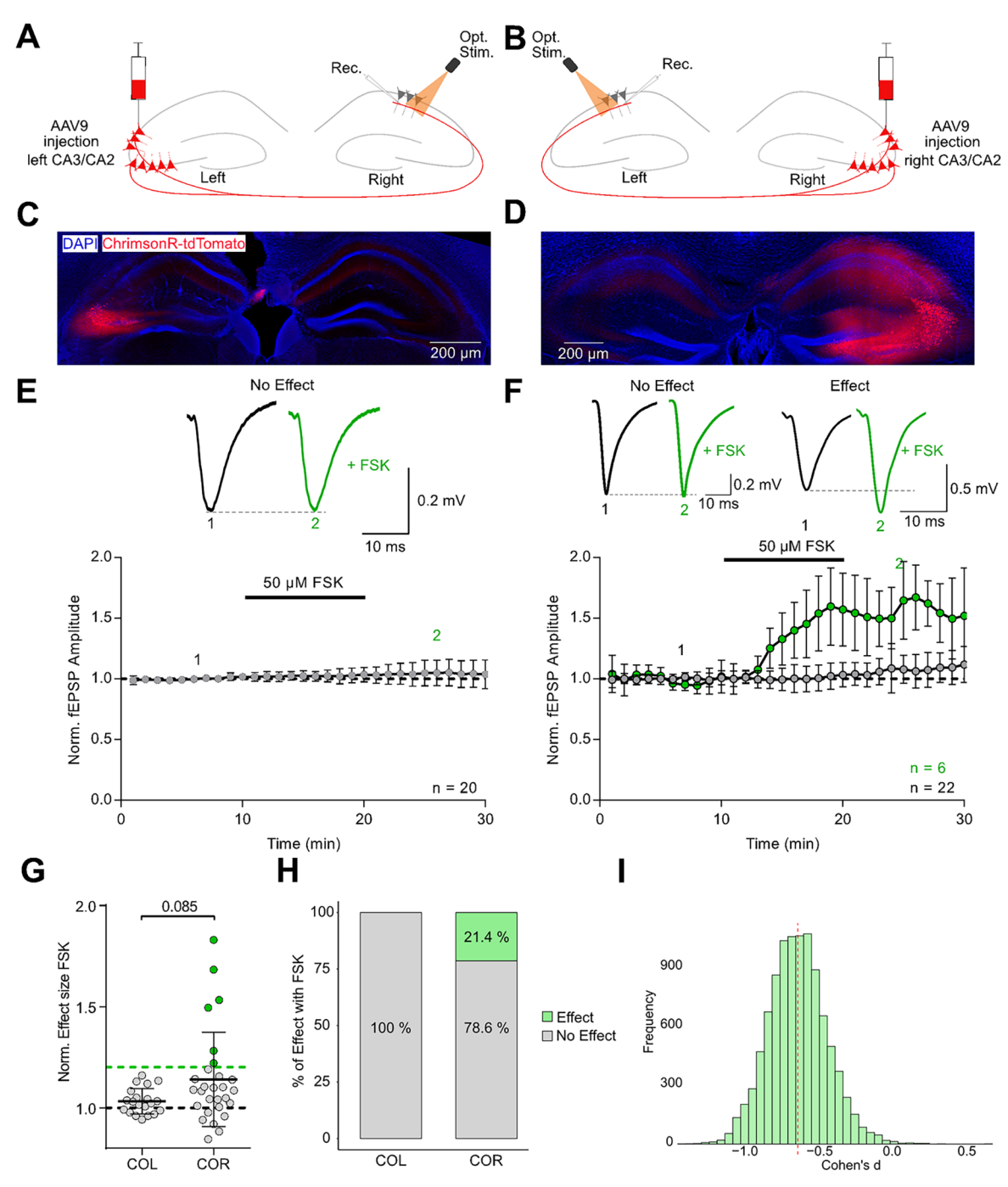


Figure 3. cAMP selectively enhances transmission at synapses formed by commissures originating from the right. A, B Optogenetic setup for stimulating commissural fibers originating from the left (COL, A) or right (COR, B) hippocampus. C, D Fluorescent images of ChrimsonR-tdTomato expression in CA3/CA2 pyramids of the left (C) and right (D) hemisphere. E, F Representative traces and timeplot of fEPSPs evoked by optogenetic stimulation of synapses formed by COL (E) and COR (F). Black traces represent baseline responses; green traces show post-FSK responses. Time course plots distinguish effect recordings (>20% increase, green) from noneffect recordings (gray). G Group summary of normalized fEPSP amplitudes illustrates a selective occurrence of FSK-induced potentiation of transmission at synapses formed by COR (p = 0.085, Mann—Whitney test). H Percent stacked bar plot categorizing individual recordings based on the presence or absence of a >20% increase in synaptic strength. No recordings from the left hemisphere met this criterion, while 6 out of 28 recordings (21.4%) in the right hemisphere showed a pronounced cAMP effect. I Distribution of bootstrapped Cohen's d values comparing left and right hemisphere responses indicates a medium effect size (Cohen's d = -0.591), suggesting a hemispheric difference.

(mean effect: $138.3 \pm 6.9\%$, n = 7), while the remaining recordings showed no effect (99.5 ± 2%, n = 22, N = 15) (Figure 1C,F). In contrast, none of the 28 recordings from the right hemisphere surpassed the 20% threshold (overall mean: 99.6 ± 9.5%, n = 28, N = 15) (Figure 1D,F). Statistical comparison confirmed a significant difference in FSK

responses between hemispheres (p = 0.018, unpaired t test with Welch's correction, Figure 1E). To further quantify this effect, we used a bootstrap approach to calculate Cohen's d, yielding a mean value of 0.664, indicative of a medium effect size and supporting the distinction between the two hemispheric data sets (Figure 1G). The paired-pulse ratio (PPR) of

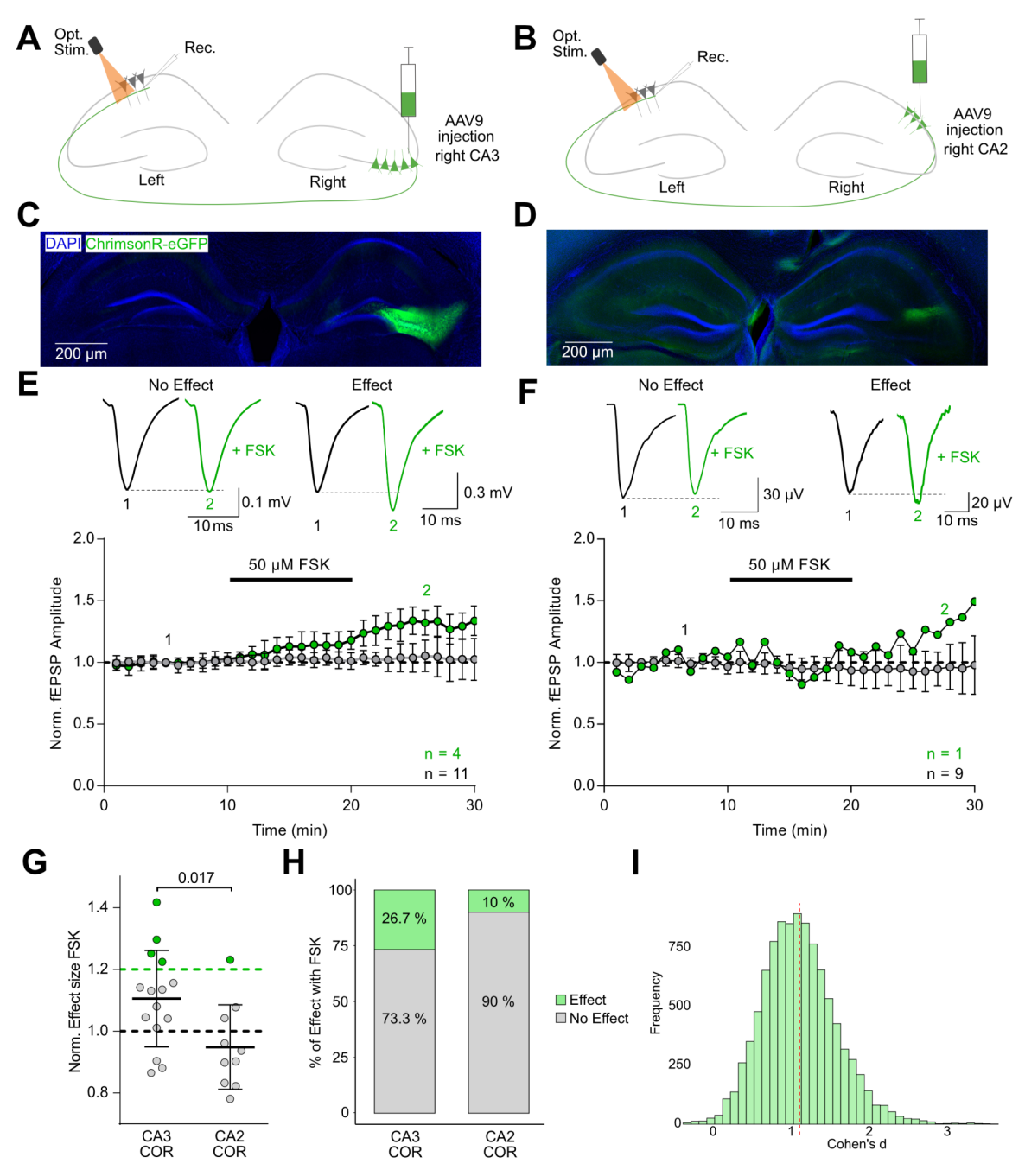


Figure 4. cAMP-induced potentiation is specific to a subset of CA3 commissures originating from the right (COR). A, B Schematic of optogenetic stimulation targeting right-hemisphere CA3 (A) or CA2 (B) pyramidal neurons using G32-4-Cre and Amigo2-Cre mice, respectively. C, D Fluorescence images showing targeted ChrimsonR-eGFP expression in CA3 (C) and CA2 (D) regions, with DAPI counterstaining for cell nuclei. E, F Representative optogenetically evoked fEPSP traces evoked by optical stimulation of commissures originating from the right CA3 (E) and right CA2 (F). Black traces represent baseline responses; green traces show post-FSK responses. Time course plots from CA3 (E) and CA2 (F) commissural recordings. Time courses highlight recordings with >20% potentiation (green) versus nonresponders (gray), underscoring the higher variability and responsiveness in the CA3 group. G Summary of normalized fEPSP amplitudes in response to 50 μ M FSK reveals significantly greater potentiation in recordings from CA3-derived commissural projections compared to CA2 (p = 0.017, unpaired t test). H Percent stacked bar plot categorizing recordings by response magnitude. In the CA2 group, only 1 of 10 recordings (10%) exceeded the 20% potentiation threshold. In contrast, 4 of 15 CA3 recordings (26.7%) showed pronounced potentiation, highlighting greater variability and a distinct subpopulation of responsive inputs. I Bootstrapped distribution of Cohen's d effect sizes comparing CA3 and CA2 responses indicates a large effect (Cohen's d = 1.138), supporting a functional distinction favoring CA3 COR.

fEPSPs evoked at a short time interval can serve as indicator for presynaptic release probability, and a change in release probability often correlates with altered PPR. In our recordings, the PPR of electrically evoked fEPSPs did not differ between right and left CA1, suggesting an overall similar release probability for CA1 inputs in both hemispheres (Figure S1A). In recordings with a >20% increase of fEPSP by FSK, PPR decreased, hinting toward a presynaptic localization of the FSK effect (Figure S1B). Together, these results reveal a clear variability in cAMP responsiveness, with FSK enhancing

synaptic transmission only in a subset of left hemisphere recordings. The absence of comparable effects in the right hemisphere suggests a lateralized expression of cAMP-dependent plasticity. Electrical stimulation activates both Schaffer collateral and commissural inputs to CA1, raising the question of whether the observed potentiation is specifically mediated by one of these pathways.

Selective Activation of Commissural Fibers Reveals Asymmetric cAMP Modulation. To dissect both hemisphere- and pathway-specific effects of cAMP signaling, we employed optogenetic activation of Schaffer collateral and commissural inputs using the channelrhodopsin ChrimsonR (K176R).²¹ An AAV9 vector encoding Syn-ChrimsonRtdTomato was unilaterally injected into either the left (Figure 2A) or right (Figure 2B) CA3/CA2 region of wild-type (WT) mice. Three to 5 weeks postinjection, acute hippocampal slices were prepared, and ChrimsonR expression was verified via tdTomato fluorescence (Figure 2C,D). Synaptic responses were recorded in CA1 stratum radiatum, either ipsilaterally or contralaterally to the injection site, using brief 590 nm light pulses (0.5-2 ms, 2-4 mW/mm²) delivered via the objective near the recording electrode at 0.1 Hz. We first evaluated the effect of cAMP elevation on Schaffer collateral synapses. Bath application of FSK failed to induce consistent potentiation in either hemisphere. In the left hippocampus, none of the recordings (0 out of 9) surpassed the 20% threshold (mean response: $103.0 \pm 7.1\%$, n = 9, N = 4, Figure 2E,H). Similarly, in the right hemisphere, 19 of 20 recordings showed no effect (mean: 99.9 \pm 9.9%), while one recording (5.3%) exhibited an increase of synaptic transmission above the threshold (124.5 ± 8.4%) (Figure 2F,H). Although a single right hemisphere recording showed a >20% increase, statistical analysis revealed no significant difference in overall FSK responses between both hemispheres (p = 0.415, unpaired t test, Figure 2G). A bootstrap analysis of effect size yielded a Cohen's d of 0.354, indicating a small effect and reflecting the marginal difference between groups (Figure 2I). These findings suggest that Schaffer collateral pathways generally lack robust cAMP sensitivity in both hemispheres.

In contrast, optogenetic activation of commissural fibers revealed substantial variability in cAMP responsiveness, particularly depending on the hemisphere of origin. At commissures originating from the left (COL) and terminating at the right hemisphere CA1 (Figure 3A,C), FSK application failed to elicit potentiation exceeding the 20% threshold in any of our recordings (mean response: $103.2 \pm 6.4\%$, n = 20, N =5; Figure 3E,H). This lack of effect was consistent across all recordings, indicating minimal variability within this group. Conversely, commissures originating from the right (COR) displayed much greater heterogeneity (Figure 3B,D). While the group mean was only modestly elevated (114.0 \pm 23.4%, n = 28, N = 11; Figure 3G), this was driven by a subset of recordings that showed strong potentiation. Specifically, 6 out of 28 recordings from COR (21.4%) exceeded the 20% effect threshold (mean: $155.6 \pm 6.3\%$). The remaining 22 recordings (78.6%) exhibited no change (mean: $107.0 \pm 2.8\%$), highlighting a substantial inter-recording variability (Figure 3F,H). A statistical comparison of overall responses revealed a trend toward greater cAMP sensitivity in COR projections (p = 0.085, unpaired t test; Figure 3G), although this did not reach conventional significance. To better capture the effect despite this variability, we conducted a bootstrap analysis, which yielded a Cohen's d of -0.591, indicative of a medium

effect size and suggesting a functional asymmetry between the commissural fibers of both hemispheres (Figure 3I). Optically evoked release displayed a reduced paired pulse facilitation compared to electrically evoked responses (Figure S1C), and the FSK-induced increase of optically evoked fEPSPs did not correlate well with decrease of the paired pulse ratio (Figure S1D). Notably, the presence of both strongly responsive and nonresponsive recordings within the COR suggests that not all COR projections are sensitive to cAMP. This variability likely reflects differences in the underlying cellular sources of these projections. Since AAV-driven ChrimsonR-tdTomato expression in WT mice lacks specificity for distinct pyramidal subtypes, the observed variability raises the possibility that the subset of cAMP-sensitive commissural fibers originate from a specific group of pyramidal neurons in the right hemisphere. Determining the identity of these responsive cells will be essential for understanding the basis of this asymmetric and heterogeneous plasticity.

CA3, but Not CA2, Commissural Projections Exhibit cAMP-Dependent Potentiation. To further pinpoint the origin of commissural fibers underlying FSK-sensitive potentiation, we employed two Cre-driver mouse lines for specific hippocampal pyramidal subpopulations, namely G32-4 Cre for CA3 and Amigo2-Cre for CA2 pyramidal neurons. Based on our earlier findings indicating hemispheric asymmetry, we focused on COR. Recording conditions were consistent with previous optogenetic experiments (Figure 4A,B). To achieve subfield-specific expression, AAV9-Synflex-rc-ChrimsonR-eGFP was injected into either CA3 or CA2 of the right hemisphere (Figure 4C,D). CA3 COR exhibited notable variability in FSK responses. While the overall mean increase was moderate (110.6 \pm 15.6%, n = 15, N = 5), this reflected again a bimodal distribution: 4 out of 15 recordings (26.7%) surpassed the 20% potentiation threshold (mean: $128.8 \pm 4.6\%$), while the remaining 11 recordings (73.3%) showed minimal to no change (mean: $103.5 \pm 1.1\%$; Figure 4E,H). This pronounced variability reflects the heterogeneity of cAMP sensitivity observed in recordings from COR in WT mice, reinforcing the hypothesis that a subpopulation of CA3 neurons is responsible for the cAMP-sensitive component of commissural transmission. In contrast, recordings from CA2 COR revealed minimal cAMP responsiveness. FSK application did not produce potentiation above the 20% threshold in 9 of 10 recordings (mean: $91.7 \pm 12.1\%$). Only one recording (10%) exhibited a substantial increase in synaptic transmission $(123.2 \pm 15.5\%)$, resulting in a modest overall group mean $(94.9 \pm 13.7\%, n = 10, N = 4; Figure 4F,H)$. The lack of strong responses across most recordings suggests limited variability and a general insensitivity of CA2-originating commissures to cAMP modulation. Although one CA2-derived recording did show potentiation, statistical comparison of overall responses revealed a significant difference between CA2 and CA3 commissural inputs (p = 0.017, unpaired t test; Figure 4G), favoring CA3 as the origin of cAMP-sensitive pathways. A bootstrap analysis further supported this distinction, yielding a Cohen's d of 1.138, indicative of a large effect size and strong functional divergence between these two subfields (Figure 4I). Together, these findings identify CA3 COR as the likely source of the variable yet pronounced cAMP-dependent potentiation observed at commissural synapses in the left CA1.

DISCUSSION

In this study, we investigated cAMP-dependent plasticity of transmission at glutamatergic synapses in mouse CA1 and found that potentiation was asymmetrically distributed across hemispheres—specifically enhancing transmitter release from commissures originating from the right hippocampus. This lateralization underscores a nuanced role for interhemispheric hippocampal communication in supporting hemispherespecific contributions to cognition.

The specificity and variability of the cAMP-induced potentiation likely reflect the underlying heterogeneity of the hippocampal circuitry. Pyramidal neurons in both CA3 and CA1 are increasingly recognized as heterogeneous populations, structured along multiple spatial axes—transverse (proximaldistal), radial (superficial-deep), and longitudinal (dorsalventral). Recent transcriptomic, anatomical, and physiological studies have revealed that subpopulations of CA1 and CA3 neurons differ markedly in gene expression, intrinsic excitability, afferent input, and functional output. 23-26 Similarly, CA3 pyramidal cells vary significantly along the proximodistal axis, with CA3b neurons exhibiting strong recurrent excitation and weaker inhibition, favoring synchronous network activity.²⁵ Morphological and electrophysiological distinctions between thorny and athorny pyramidal neurons further reveal subtypes with differing input sources and roles in sharp-wave ripple initiation.²⁷ Such cellular diversity within CA3 likely shapes the input specificity and variability observed in commissural plasticity. Analysis of the ChrimsonR-expression pattern in slices from mice exhibiting FSK effects did not reveal any localized cluster of CA3 cells that could be categorized as a distinct group providing enhanced FSK sensitivity (Figure S2A). If the effect were strictly input side-dependent, one would expect larger FSK effects in the commissural pathway originating from the right hemisphere to correlate with larger effects in the Schaffer collateral pathway in the right hemisphere within the same animal. Our data set contains measurements from three animals in which both pathways were tested (Figure S2C). Within these recordings, no meaningful correlation can be drawn. Adding a molecular layer of complexity, adenylyl cyclase isoforms—the enzymes responsible for cAMP production—are differentially expressed and regulated across hippocampal neurons.²⁸ This spatial heterogeneity in cAMP synthesis may contribute to preferential activation of cAMP signaling cascades in distinct cell types and subcellular compartments. Even modest presynaptic modulation via cAMP could yield significant functional changes when coupled with postsynaptic reinforcement mechanisms, as suggested by the cooperative model of LTP, ²⁹ emphasizing the synergistic role of presynaptic neurotransmitter release and postsynaptic AMPA receptor insertion in sustaining plasticity. However, as we consistently used low frequency (0.1 Hz) stimulation for evoking transmitter release, it seems unlikely that postsynaptic depolarization unlocked plasticity-mechanisms that could act synergistically with FSK/cAMP. Noncircuit-related factors such as age and sex could also contribute to the observed variability. Synaptic plasticity is generally more pronounced at early developmental stages than in later life, 30,31 yet we did not detect any differences in FSK responsiveness between juvenile (<12 weeks) and young adult (>12 weeks) animals (Figure S3B) across all recordings. In recordings of optically evoked transmission from COR, young adults tended to show slightly

stronger responses to FSK, but the effect was not significant. Estrogen signaling has been implicated in sex-specific regulation of LTP.³² Considering data from all experiments, we found FSK-mediated potentiation in both sexes, and observed no difference in FSK effect size between male and female animals (Figure S3C). However, looking specifically on the WT COR recordings we detected stronger FSK effects in males (Figure S3E). Finally, to address the possibility that hemispheric differences in fEPSPs reflected unequal baseline transmitter release, we assessed release probability using paired-pulse ratio (PPR) during baseline recordings. No significant hemispheric differences in PPR were observed, but optical stimulation yielded generally lower PPR (Figure S1A,B). Forskolin-induced potentiation was associated with paired-pulse depression in recordings with electrical stimulation (Figure S1B), but this relationship was not consistent for optically stimulated COR inputs (Figure S1D), potentially due to overbouton stimulation, which can obliterate PPR dynamics.²² Together, our results indicate that the observed differences in FSK responsiveness are unlikely to originate from age, sex, or baseline release probability. The adaptive significance of commissural plasticity is especially compelling in light of its lateralization. While often overshadowed by ipsilateral hippocampal pathways, commissural projections are essential for coordinating activity between hemispheres. The asymmetric nature of the cAMP-mediated potentiation observed here mirrors structural and functional lateralization in the hippocampus. Behavioral studies in rodents have linked paw preference to hemispheric differences in mossy fiber projections and learning strategies.^{33,34} Human split-brain studies revealed that commissural pathways are critical for the integration of memory, perception, and executive function.³⁵ Genetic models with disrupted forebrain commissures also demonstrate impairments in memory consolidation,³⁶ supporting the role of interhemispheric communication in cognition. Lateralized synaptic plasticity may thus enable functional specialization between hemispheres. For instance, Jordan et al.³⁷ propose that asymmetric plasticity could underlie divergent spatial and contextual processing roles in left and right hippocampi. In this context, plasticity at commissural synapses may fine-tune bilateral coordination and enable flexible behavior in response to complex environments.

In summary, our findings demonstrate that commissural projections can engage cAMP-dependent plasticity in a hemisphere-specific manner, likely driven by the interaction of diverse neuronal subpopulations and spatially restricted molecular signaling. This form of plasticity may serve not only as a mechanism for synaptic modulation but also as a substrate for lateralized memory encoding and interhemispheric integration. Future investigations using refined cell-type- and projection-specific manipulations will be essential to unravel how commissural plasticity shapes hippocampal function and contributes to cognition.

METHODS

Animals. All experiments were conducted in accordance with Directive 2010/63/EU on the protection of animals used for scientific purposes and approved by the Berlin state authorities (LAGeSo; license numbers G0030/20, T0100/03). Mice were bred at the Charité animal facility and housed in individually ventilated cages (4–10 per cage) under a 12-h light—dark cycle with *ad libitum* access to food and water. Mice of either sex were used from the following lines: Wild-type animals (C57BL/6N), Amigo2-Cre (RRID:IMSR_-JAX:030215; obtained from Jackson Laboratory with a C57BL/6 ×

CBA background), and Grik4-Cre (RRID:IMSR_JAX:006474; obtained from Jackson Laboratory with a C57BL/6 background). Transgenic lines were genotyped according to established protocols, and hemizygous mice were crossed with C57BL/6N mice over several generations, minimizing genetic background differences between the lines.

Stereotactic Viral Injection. Stereotactic injections were performed using a Neurostar half-automated system. Mice received Metamizol (200 mg/kg bodyweight) in drinking water 1 day before and 3 days after surgery. Mice were anesthetized with 5% isoflurane, maintained at 1.5-2% throughout surgery. After scalp disinfection and local lidocaine administration, craniotomies were performed. Injection coordinates were: CA3: AP -1.75 mm, ML 2.1 mm, DV 2.18 mm, CA2: AP -1.75 mm, ML 2.05 mm, DV 1.80 mm. AAV9 (200-400 nL) encoding Syn-ChrimsonR-tdTomato or Syn-flex-rc-ChrimsonR-GFP (Addgene #59171 and #84480, a kind gift from Edward Boyden) was injected into area CA3 or CA2 via a Hamilton syringe at 40-100 nL/min, followed by a 5 min wait before needle retraction. Mice received Carprofen (5 mg/kg bodyweight) postsurgery, and NaCl was administered subcutaneously if procedures exceeded 1 h. The scalp was sutured, sanitized, and mice were monitored on a heating pad before returning to their home cages.

Acute Brain Slice Preparation. Acute coronal hippocampal slices (300 μ m) were obtained from 6–18-week-old mice (WT: 6–15 weeks; G32-4 Cre: 9-13 weeks; Amigo2 Cre: 10-18 weeks) from both sexes. Following deep anesthesia with isoflurane, mice were decapitated, and brains were rapidly transferred to ice-cold, oxygenated sucrose-based artificial cerebro spinal fluid (S-aCSF), containing: 124 mM NaCl, 3 mM KCl, 3 mM MgCl₂, 0.5 mM CaCl₂, 1.25 mM NaH₂PO₄, 26 mM NaHCO₃, 10 mM glucose, 243 mM sucrose. After a 3 min incubation, the brain was mounted on a Leica VT1200S vibratome for slicing under continuous ice-cold S-aCSF perfusion. Following dissection, the hemispheres were separated, and a cortical cut was introduced in the left hemisphere to enable reliable identification of laterality. Slices were transferred to a 32 °C oxygenated S-aCSF holding chamber for 30 min, then allowed to recover in a second chamber with aCSF for ≥ 1 h before recordings, containing: 124 mM NaCl, 3 mM KCl, 1.5 mM MgCl₂, 2.5 mM CaCl₂, 1.25 mM NaH₂PO₄, 26 mM NaHCO₃, and 10 mM glucose.

Electrophysiology. Slices were transferred to a submerged recording chamber perfused with oxygenated aCSF (2–3 mL/min, room temperature). Glass electrodes (1–2 $\mathrm{M}\Omega$) filled with aCSF were positioned in CA1 stratum radiatum for field fEPSP recordings. Cells were visualized via IR-DIC microscopy, and recordings were obtained using a MultiClamp 700B amplifier. Schaffer collaterals were stimulated via a bipolar electrode, delivering paired pulses with 40 ms interstimulus interval at 0.1 Hz. Stimulation strength was set to elicit 40–50% of the maximum fEPSP amplitude. Signals were amplified, low-pass filtered (3 kHz), digitized (10 kHz) using a Digidata 1440A, and recorded using pClamp10.

Optogenetic Stimulation. Photostimulation was achieved using a pE300 CoolLED light source, coupled to an Olympus BX51WI microscope via a liquid light guide and filtered by a HC-Tripleband 365-380/470/585 filter (AHF F66-L422). Synaptic responses were evoked by paired 590 nm light pulses at 0.1 Hz (0.5–2 ms flash duration, 40 ms interval, 1–6 mW/mm², 40× objective [Olympus LUMPL FLN 40XW Objective]).

Data Analysis. Electrophysiological data were analyzed offline using AxoGraph X and GraphPad Prism 6. Baseline normalization, a 1 kHz low-pass filter, and fEPSP amplitude detection were performed in AxoGraph X. Data normality was assessed using the Shapiro—Wilk test. Statistical analyses were generated in GraphPad Prism 6, with results expressed as mean \pm SD. N refers to the number of animals used per experiment, and n denotes the number of individual recordings. Graphical representations were generated in GraphPad Prism 6 and Affinity Designer 2. To quantify the standardized difference between two independent groups, we calculated Cohen's d and estimated its sampling distribution using nonparametric bootstrapping. The bootstrap procedure involved resampling with replacement from each group's data to generate 10 000 paired

bootstrap samples. For each iteration, Cohen's d was computed as the difference in means divided by the pooled standard deviation. This process was repeated 10 000 times to construct a distribution of Cohen's d values. The mean of the bootstrap distribution was taken as the point estimate of the effect size. All analyses and visualizations were conducted using R (version 4.1.1) with the *boot* and *ggplot2* packages.

Image Analysis of the Cell-Expression Pattern. Fluorescent images of ChrimsonR expression (TIFF files) were processed in R (version 4.1.1) using EBImage (Bioconductor) and tidyverse packages. For each image, the red channel was isolated and normalized to a [0,1] scale. A global threshold was applied to the normalized pixel intensities. Pixels above threshold were segmented into connected components. For each component, centroid coordinates (x,y), pixel area, and mean red intensity were computed using *computeFeatures.moment* and *computeFeatures.basic* (EBImage). For visualization, centroids were normalized to unit coordinates relative to image width and height, and plotted as points whose size and color scale with mean intensity. Figures were generated with ggplot2 plotting in R.

ASSOCIATED CONTENT

Data Availability Statement

The datasets used and/or analyzed during the current study are available from the corresponding author upon request.

5 Supporting Information

The Supporting Information is available free of charge at https://pubs.acs.org/doi/10.1021/acschemneuro.5c00454.

Release probability across hemispheres and correlation with FSK responsiveness in WT animals; variable viral expression in CA3 and individual display of forskolin effects detailed breakdown; and no correlation of age or sex with FSK responsiveness (PDF)

AUTHOR INFORMATION

Corresponding Authors

Dietmar Schmitz – German Center for Neurodegenerative Diseases (DZNE), Berlin 10117, Germany; Institute of Cell Biology and Neurobiology, and Neuroscience Research Center, Charité-Universitätsmedizin Berlin, Corporate Member of Freie Universität Berlin and Humboldt-Universität Zu Berlin, Berlin 10117, Germany; Bernstein Center for Computational Neuroscience, Humboldt Universität Zu Berlin, Berlin 10115, Germany; Email: dietmar.schmitz@charite.de

Benjamin R. Rost — German Center for Neurodegenerative Diseases (DZNE), Berlin 10117, Germany; Institute of Cell Biology and Neurobiology, and Neuroscience Research Center, Charité-Universitätsmedizin Berlin, Corporate Member of Freie Universität Berlin and Humboldt-Universität Zu Berlin, Berlin 10117, Germany; Email: benjamin.rost@dzne.de

Authors

Lukas Faiss — German Center for Neurodegenerative Diseases (DZNE), Berlin 10117, Germany; Institute of Cell Biology and Neurobiology, and Neuroscience Research Center, Charité-Universitätsmedizin Berlin, Corporate Member of Freie Universität Berlin and Humboldt-Universität Zu Berlin, Berlin 10117, Germany; orcid.org/0000-0001-5150-5541

Aikaterini Salivara — German Center for Neurodegenerative Diseases (DZNE), Berlin 10117, Germany; Institute of Cell Biology and Neurobiology, and Neuroscience Research Center, Charité-Universitätsmedizin Berlin, Corporate Member of Freie Universität Berlin and Humboldt-Universität Zu Berlin, Berlin 10117, Germany

Silvia Oldani – Maxwell Biosystems, Zürich 8047, Switzerland Jörg Breustedt – Institute of Cell Biology and Neurobiology, and Neuroscience Research Center, Charité-Universitätsmedizin Berlin, Corporate Member of Freie Universität Berlin and Humboldt-Universität Zu Berlin, Berlin 10117, Germany

Complete contact information is available at: https://pubs.acs.org/10.1021/acschemneuro.5c00454

Author Contributions

L.F., A.S., and S.O. performed the experiments. L.F. and B.R.R. analyzed the data. B.R.R., D.S., and J.B. conceptualized the research. B.R.R. and D.S. acquired funding for the project. B.R.R., D.S., and J.B. supervised the work. L.F. and B.R.R. wrote the paper with input from all authors. All authors approved the submission of the manuscript.

Funding

This work was supported by grants from the European Commission (ERC "BrainPlay", project-ID. 810580, to D.S.), the Einstein Foundation (D.S.), and the German Research Foundation (Deutsche Forschungsgemeinschaft, DFG): Germany's Excellence Strategy-EXC 2049 (NeuroCure, project-ID. 390688087, D.S.), SPP1926 ("Next generation optogenetics", project-ID. 425994138, to B.R.R.), and SFB1315 ("Mechanisms and Disturbances in Memory Consolidation: From Synapses to Systems", project-ID. 327654276, to D.S. and B.R.R.).

Notes

The authors declare no competing financial interest.

■ ACKNOWLEDGMENTS

The authors thank Anke Schönherr, Susanne Rieckmann, Anny Kretschmer, and Katja Czieselsky for excellent technical assistance, and the viral core facility (VCF) of the Charité for providing AAVs.

ABBREVIATIONS

COL commissures originating from the left COR commissures originating from the right fEPSPs field excitatory postsynaptic potentials

FSK forskolin
iv inversus viscerum
LTP long-term potentiation
PPR paired pulse ratio

REFERENCES

- (1) Blackstad, T. W. Commissural connections of the hippocampal region in the rat, with special reference to their mode of termination. *J. Comp. Neurol* **1956**, *105* (3), 417–537.
- (2) Andersen, P.; Blackstad, T. W.; Lömo, T. Location and identification of excitatory synapses on hippocampal pyramidal cells. *Exp. Brain Res* **1966**, *1* (3), 236–248.
- (3) Gottlieb, D. I.; Cowan, W. M. Autoradiographic studies of the commissural and ipsilateral association connections of the hippocampus and dentate gyrus. I. The commissural connections. *J. Comp. Neurol* 1973, 149 (4), 393–421.
- (4) Swanson, L. W.; Wyss, J. M.; Cowan, W. M. An autoradiographic study of the organization of intrahippocampal association pathways in the rat. *J. Comp. Neurol* **1978**, *181* (4), 681–715.

- (5) Kawakami, R.; Shinohara, Y.; Kato, Y.; Sugiyama, H.; Shigemoto, R.; Ito, I. Asymmetrical allocation of NMDA receptor $\varepsilon 2$ subunits in hippocampal circuitry. *Science* **2003**, *300* (5621), 990–994.
- (6) Shinohara, Y.; Hirase, H.; Watanabe, M.; Itakura, M.; Takahashi, M.; Shigemoto, R. Left-right asymmetry of the hippocampal synapses with differential subunit allocation of glutamate receptors. *Proc. Natl. Acad. Sci. U. S. A* 2008, 105 (24), 19498–19503.
- (7) Kawakami, R.; Dobi, A.; Shigemoto, R.; Ito, I. Right isomerism of the brain in inversus viscerum mutant mice. *PLoS One* **2008**, 3 (4), No. e1945.
- (8) Goto, K.; Kurashima, R.; Gokan, H.; Inoue, N.; Ito, I.; Watanabe, S. Left–Right Asymmetry Defect in the Hippocampal Circuitry Impairs Spatial Learning and Working Memory in iv Mice. *PLoS One* **2010**, *5* (11), No. e15468.
- (9) Klur, S.; Muller, C.; Pereira de Vasconcelos, A.; Ballard, T.; Lopez, J.; Galani, R.; et al. Hippocampal-dependent spatial memory functions might be lateralized in rats: An approach combining gene expression profiling and reversible inactivation. *Hippocampus* **2009**, 19 (9), 800–816.
- (10) Benito, N.; Martin-Vazquez, G.; Makarova, J.; Makarov, V. A.; Herreras, O. The right hippocampus leads the bilateral integration of gamma-parsed lateralized information. *elife* **2016**, *5*, No. e16658.
- (11) Kohl, M. M.; Shipton, O. A.; Deacon, R. M.; Rawlins, J. N. P.; Deisseroth, K.; Paulsen, O. Hemisphere-specific optogenetic stimulation reveals left-right asymmetry of hippocampal plasticity. *Nat. Neurosci* **2011**, *14* (11), 1413–1415.
- (12) Shipton, O. A.; El-Gaby, M.; Apergis-Schoute, J.; Deisseroth, K.; Bannerman, D. M.; Paulsen, O.; et al. Left-right dissociation of hippocampal memory processes in mice. *Proc. Natl. Acad. Sci. U. S. A* **2014**, *111* (42), 15238–15243.
- (13) El-Gaby, M.; Shipton, O. A.; Paulsen, O. Synaptic Plasticity and Memory: New Insights from Hippocampal Left Right Asymmetries. *Neurosci* **2015**, 21 (5), 490–502.
- (14) Fan, L. Z.; Kim, D. K.; Jennings, J. H.; Tian, L.; Wang, P. Y.; Ramakrishnan, C.; Randles, S.; Sun, Y.; Thadhani, E.; Kim, Y. S.; et al. Article All-optical physiology resolves a synaptic basis for behavioral timescale plasticity ll All-optical physiology resolves a synaptic basis for behavioral timescale plasticity. *Cell* **2023**, *186* (3), 543–559.e19.
- (15) Martin, S. J.; Shires, K. L.; da Silva, B. M. Hippocampal Lateralization and Synaptic Plasticity in the Intact Rat: No Left—Right Asymmetry in Electrically Induced CA3-CA1 Long-Term Potentiation. *Neuroscience* **2019**, *397*, 147–158.
- (16) Kuwajima, M.; Ostrovskaya, O. I.; Cao, G.; Weisberg, S. A.; Harris, K. M.; Zemelman, B. V. Ultrastructure of light-activated axons following optogenetic stimulation to produce late-phase long-term potentiation. *PLoS One* **2020**, *15* (1), No. e0226797.
- (17) Bernabeu, R.; Bevilaqua, L.; Ardenghi, P.; Bromberg, E.; Schmitzt, P.; Bianchin, M.; Izquierdo, I.; Medina, J. H. Involvement of hippocampal cAMP/cAMP-dependent protein kinase signaling pathways in a late memory consolidation phase of aversively motivated learning in rats. *Proc. Natl. Acad. Sci. U. S. A* 1997, 94 (13), 7041–7046
- (18) Otmakhova, N. A.; Otmakhov, N.; Mortenson, L. H.; Lisman, J. E. Inhibition of the cAMP pathway decreases early long-term potentiation at CA1 hippocampal synapses. *J. Neurosci* **2000**, *20* (12), 4446–4451.
- (19) Otmakhov, N.; Khibnik, L.; Otmakhova, N.; Carpenter, S.; Riahi, S.; Asrican, B.; et al. Forskolin-Induced LTP in the CA1 Hippocampal Region Is NMDA Receptor Dependent. *J. Neurophysiol* **2004**, *91* (5), 1955–1962.
- (20) Muñoz, M.-D.; Solís, J. M. Characterisation of the mechanisms underlying the special sensitivity of the CA2 hippocampal area to adenosine receptor antagonists. *Neuropharmacology* **2019**, *144*, 9–18.
- (21) Klapoetke, N. C.; Murata, Y.; Kim, S. S.; Pulver, S. R.; Birdsey-Benson, A.; Cho, Y. K.; et al. Independent optical excitation of distinct neural populations. *Nat. Methods* **2014**, *11* (3), 338–346.
- (22) Jackman, S. L.; Beneduce, B. M.; Drew, I. R.; Regehr, W. G. Achieving high-frequency optical control of synaptic transmission. *J. Neurosci* **2014**, *34* (22), 7704–7714.

- (23) Mizuseki, K.; Diba, K.; Pastalkova, E.; Buzsáki, G. Hippocampal CA1 pyramidal cells form functionally distinct sublayers. *Nat. Neurosci* **2011**, *14* (9), 1174–1183.
- (24) Cembrowski, M. S.; Bachman, J. L.; Wang, L.; Sugino, K.; Shields, B. C.; Cembrowski, M. S.; et al. Spatial Gene-Expression Gradients Underlie Prominent Heterogeneity of CA1 Pyramidal Neurons Article Spatial Gene-Expression Gradients Underlie Prominent Heterogeneity of CA1 Pyramidal Neurons. *Neuron* **2016**, 89 (2), 351–368.
- (25) Sun, Q.; Sotayo, A.; Cazzulino, A. S.; Snyder, A. M.; Denny, C. A.; Siegelbaum, S. A. Proximodistal Heterogeneity of Hippocampal CA3 Pyramidal Neuron Intrinsic Properties, Connectivity, and Reactivation during Memory Recall. *Neuron* **2017**, 95 (3), 656–672.e3.
- (26) Cembrowski, M. S.; Spruston, N. Heterogeneity within classical cell types is the rule: lessons from hippocampal pyramidal neurons. *Nat. Rev. Neurosci.* **2019**, *20*, 193–204.
- (27) Hunt, D. L.; Linaro, D.; Si, B.; Romani, S.; Spruston, N. A novel pyramidal cell type promotes sharp-wave synchronization in the hippocampus. *Nat. Neurosci* **2018**, *21* (July), 985.
- (28) Shahoha, M.; Cohen, R.; Ben-Simon, Y.; Ashery, U. cAMP-Dependent Synaptic Plasticity at the Hippocampal Mossy Fiber Terminal. *Front. Synaptic Neurosci.* **2022**, *14*, 861215.
- (29) Lisman, J.; Raghavachari, S. A Unified Model of the Presynaptic and Post- synaptic Changes During LTP at CA1 Synapses. *Science* **2006**, 2006, rel1.
- (30) Lehmann, K.; Löwel, S. Age-dependent ocular dominance plasticity in adult mice. *PLoS One* **2008**, *3* (9), No. e3120.
- (31) Hübener, M.; Bonhoeffer, T. Neuronal plasticity: Beyond the critical period. *Cell* **2014**, *159* (4), *727*–*737*.
- (32) Wang, W.; Le, A. A.; Hou, B.; Lauterborn, J. C.; Cox, C. D.; Levin, E. R.; et al. Memory-related synaptic plasticity is sexually dimorphic in rodent hippocampus. *J. Neurosci* **2018**, *38* (37), 7935–7951.
- (33) Collins, R. L. When left-handed mice live in right-handed worlds. *Science* **1975**, *187* (4172), *181*–184.
- (34) Lipp, H. P.; Collins, R. L.; Hausheer-Zarmakupi, Z.; Leisinger-Trigona, M. C.; Crusio, W. E.; Nosten-Bertrand, M.; et al. Paw preference and intra-/infrapyramidal mossy fibers in the hippocampus of the mouse. *Behav. Genet* **1996**, *26* (4), 379–390.
- (35) Gazzaniga, M. S. Forty-five years of split-brain research and still going strong. *Nat. Rev. Neurosci.* **2005**, *6* (8), 653–659.
- (36) Ribeiro, A. S.; Eales, B. A.; Biddle, F. G. Short-term and long-term memory deficits in handedness learning in mice with absent corpus callosum and reduced hippocampal commissure. *Behav Brain Res* **2013**, 245, 145–151.
- (37) Jordan, J. T. The rodent hippocampus as a bilateral structure: A review of hemispheric lateralization. *Hippocampus* **2020**, *30* (3), 278–292.

